Surface shape and local critical behavior: The percolation problem in two dimensions

Bertrand Berche*
Laboratoire de Physique du Solide, Université Henri Poincaré, Nancy 1, Boîte Postale 239, F-54506 Vandœuvre lès Nancy Cedex, France

Jean-Marc Debierre†
Laboratoire MATOP, Faculté des Sciences de St Jérôme, Case 151, 13397 Marseille Cedex 20, France

Hans-Peter Eckle‡
Laboratoire de Physique du Solide, Université Henri Poincaré, Nancy 1, Boîte Postale 239, F-54506 Vandœuvre lès Nancy Cedex, France

(Received 5 July 1994)

The critical behavior of site percolation confined to the interior of a parabola is investigated. At the percolation threshold, conformal mapping is used to derive analytical expressions for the pair correlation function and the local order parameter in the case of free and fixed boundary conditions, respectively. Numerical results obtained by intensive Monte Carlo simulations are in excellent agreement with the analytical expressions. The numerical data for the off-critical local order parameter with free boundary conditions show that correction to scaling terms are important and the leading correction exponent is estimated to be $\epsilon \simeq 0.18$.

PACS number(s): 05.50.+q, 05.70.Jk, 64.60.Cn, 64.60.Fr

I. INTRODUCTION

The local critical behavior of a given system may be influenced by the shape of its surface. This effect was first noticed some years ago by Cardy [1], who studied the case of a corner or wedge geometry for which varying local exponents are obtained [2,3]. More general shapes were later considered for which the surface is located at

$$v = \pm C u^k \tag{1.1}$$

in two dimensions or in a section of the system in higher dimensions [4]. For an isotropic system, the coefficient C transforms as $C' = b^{k-1}C$ under rescaling by a factor b. When $k > 1$, iterative rescaling causes C' to diverge ultimately and the system behaves as if its surface were flat. It follows that taking the flat surface fixed point as a reference, one may consider $1/C$ as a scaling field with an anomalous dimension $y_C = 1 - k$ which is related to the surface shape. For an isotropic system, any quantity $Q(u, t, C^{-1})$ is assumed to have a generalized homogeneous form:

$$Q(u, t, C^{-1}) = b^{-x_Q} f\left(\frac{u}{b}, b^{1/\nu} t, \frac{b^{1-k}}{C}\right), \tag{1.2}$$

where t describes the deviation from the critical point, x_Q is the anomalous dimension associated with Q, and ν is the bulk correlation length exponent. The variable C plays the same role as the linear size L of a system in finite-size scaling [5]. In the corner geometry ($k = 1$), y_C vanishes so that the surface shape becomes a marginal perturbation and the local exponents depend on C which is related to the opening angle of the corner. Finally, when $k < 1$ the perturbation induced by the surface is relevant and an alternative local critical behavior is obtained.

In the past few years, a number of critical systems with the surface shape defined by Eq (1.1) have been studied. For the Ising model in two dimensions, the correlation functions between a point at the tip of the surface curve (1.1) and the bulk (tip-bulk correlation functions), and the local order parameter were shown to display a stretched exponential behavior [4,6,7]. For a confined polymer, anisotropic k-dependent exponents were obtained for the radius of gyration [8]. In the case of anisotropic critical systems, the scaling dimension y_C becomes $1 - zk$, where the dynamical exponent $z = \nu_\parallel/\nu_\perp$ is the ratio of the correlation length exponents. For the directed walk with $z = 2$ the marginal shape is the parabola and the same type of behavior as for the Ising model was obtained in the relevant case [9,10]. More recently, directed percolation was also considered [11].

In the present paper, we investigate the local critical behavior of the site percolation problem confined inside a generalized parabola as given by Eq. (1.1). In Sec. II, the correspondence between the site percolation and the q-state Potts model in the limit $q \to 1$ is used to find the expression of the local order parameter. In Sec. III, we apply conformal invariance to derive analytical results

*Electronic address: berche@lps.u-nancy.fr
†Electronic address: debierre@matop.univ-mrs.fr
‡Present address: Princeton University, Jadwin Hall, P.O. Box 708, Princeton, NJ 08544-0708. Electronic address: eckle@puhep1.Princeton.edu

at the critical point: for free boundary conditions the tip-bulk correlation function is deduced from the conformal transformation which maps the half plane onto the interior of the generalized parabola and the profile of the order parameter along the axis of the parabola is obtained for fixed boundary conditions. The algorithm used for the Monte Carlo simulations is presented in Sec. IV. The numerical results obtained at the critical point are then compared to the conformal invariance predictions in Sec. V. We eventually show in Sec. VI that corrections to scaling have to be explicitly taken into account in order to ensure satisfactory scaling for the data obtained for the off-critical profile of the order parameter. The last section gives a summary of the results.

II. POTTS MODEL AND PERCOLATION

The bond percolation problem is well known to correspond to the limit $q \to 1$ of a usual q-state Potts model [12–14], while the site problem corresponds to a Potts model with multispin interactions in the same limit [15,16]. In this section, we summarize this equivalence which enables us to write conveniently the local quantities such as the local order parameter.

Consider a lattice $\mathcal{L}$ of N sites with a coordination number z. In order to define site percolation on $\mathcal{L}$, we introduce a covering lattice $\mathcal{L}_c$ with its $\frac{1}{2}Nz$ sites located on the edges of $\mathcal{L}$ [16]. The q-state Potts variables n_i ($n_i = 0, 1, \ldots, q-1$) are located on each lattice site i of $\mathcal{L}_c$ and coupled via z-site interactions K/k_BT. The state $n_i = 0$ is, furthermore, stabilized when a magnetic field H/k_BT is applied. In order to infer local properties, one has to add a local magnetic field H_ℓ/k_BT acting on a particular site labeled ℓ which will be called the origin site hereafter. The Hamiltonian for this model is written,

$$-\beta\mathcal{H} = K\sum_i (q\delta\{n_i\} - 1) + H\sum_i (q\delta_0\{n_i\} - 1) + H_\ell(q\delta_0\{n_\ell\} - 1), \quad (2.1)$$

where $\delta\{n_i\} = 1$ if the z spins surrounding the site i of $\mathcal{L}$ are in the same state and 0 otherwise while $\delta_0\{n_i\} = 1$ if the surrounding spins are in the state 0. Defining the probability p,

$$p = 1 - e^{-qK}, \quad (2.2)$$

the partition function $\mathcal{Z}_N = \mathrm{Tr}\, e^{-\beta\mathcal{H}}$ can be written, omitting an unimportant prefactor:

$$\mathcal{Z}_N = \mathrm{Tr}\left\{(1-p)^{Nz/2}\prod_i\left(1 + \frac{p}{1-p}\delta\{n_i\}\right) \times \prod_i e^{qH(\delta_0\{n_i\}-1)} e^{qH_\ell(\delta_0\{n_\ell\}-1)}\right\}. \quad (2.3)$$

The correspondence with the percolation problem is obtained via a graph expansion, each configuration of the Potts variables being represented by a graph $\mathcal{G}$ where the sites are occupied with a probability p when neighbor spins are in the same state. The free energy of the system in the limit $q \to 1$ can be defined by

$$F(p) = \left(\frac{\partial \ln \mathcal{Z}_N}{\partial q}\right)_{q=1}, \quad (2.4)$$

thus, in the thermodynamic limit $N \to \infty$ the contribution of the infinite cluster vanishes when $H \to 0+$ and the free energy is written as a sum over finite clusters only ($\sum'$):

$$F(p) = \sum_s{}' [e^{-sH}\mathcal{N}(s) + e^{-(sH+H_\ell)}\mathcal{N}_\ell(s)], \quad (2.5)$$

where $\mathcal{N}(s)$ is the average number of clusters of s sites which do not contain the origin site, while $\mathcal{N}_\ell(s)$ is the probability that the origin site belongs to a cluster of s sites. The first term in the right hand side of equation (2.5) is the bulk contribution $F_{\mathrm{blk}}(p)$, while the second proceeds from the local term $F_\ell(p)$.

The probability of percolation $P(p)$ is then defined by the derivative of the free energy per site:

$$P(p) = \lim_{H\to 0+}\frac{\partial f_{blk}}{\partial H} = 1 - \sum_s{}' s\frac{\mathcal{N}(s)}{N}, \quad (2.6)$$

and the local order parameter is given by

$$P_\ell(p) = \lim_{\substack{H\to 0+ \\ H_\ell \to 0+}}\frac{\partial f_\ell}{\partial H_\ell} = 1 - \sum_s{}' \mathcal{N}_\ell(s). \quad (2.7)$$

The local order parameter is then the probability that the origin site belongs to the infinite cluster.

The critical exponents for the percolation problem in two dimensions can thus be deduced from the known values for the two-dimensional Potts model [14,17].

III. CONFORMAL ASPECTS

The conformal transformation,

$$z = i\cosh\left(\frac{\pi w^{1-k}}{2C(1-k)}\right), \quad (3.1)$$

is known to provide a conformal mapping of the two-dimensional half plane $z = x + iy = re^{i\varphi}$ onto the inside of a generalized parabola in the $w = u + iv = \rho e^{i\theta}$ plane [4,7]. This transformation can also be written

$$x + iy = -\sinh\alpha\,\sin\beta + i\,\cosh\alpha\,\cos\beta, \quad (3.2)$$

where we have introduced the variables

$$\alpha = \frac{\pi\rho^{1-k}}{2C(1-k)}\cos[(1-k)\theta], \qquad \beta = \frac{\pi\rho^{1-k}}{2C(1-k)}\sin[(1-k)\theta]. \quad (3.3)$$

The surface of the semi-infinite system $y = 0$ is then mapped onto a curve whose equation is a parabola when $k = 1/2$,

$$\rho(1-\cos\theta)=\frac{C^2}{2}, \tag{3.4}$$

while for other values of $k<1$, the equation of the confining surface asymptotically is

$$v=\pm Cu^k. \tag{3.5}$$

Under a conformal mapping, the correlation function at the critical point is transformed according to [18]

$$G(w_1,w_2)=b^x(z_1)b^x(z_2)G(z_1,z_2), \tag{3.6}$$

where x is the bulk magnetic exponent and the local scale factor $b(z)$ in our case is given by

$$b(z)=\left|\frac{dz}{dw}\right|=\frac{\pi}{2C\rho^k}(\sinh^2\alpha+\sin^2\beta)^{1/2}. \tag{3.7}$$

Starting from the algebraic decay of the correlation function of the semi-infinite system [1],

$$G(z_1,z_2)=\frac{1}{(y_1y_2)^x}\psi(\omega),\quad \omega=\frac{4y_1y_2}{|z_1-z_2|^2}, \tag{3.8}$$

where $\psi(\omega)$ is a scaling function, one can deduce the correlation function $G(w_1,w_2)$ in the parabolic geometry. For the correlations between the origin site and a distant site on the u axis ($\rho=u,\theta=0$), this two-point correlation function takes the simple form

$$G(u)=\left(\frac{\pi}{2C}\right)^{2x}u^{-kx}\tanh^x\left(\frac{\pi}{2C(1-k)}\right)\times\tanh^x\left(\frac{\pi u^{1-k}}{2C(1-k)}\right)\psi(\omega). \tag{3.9}$$

A stretched exponential behavior is recovered as in another context [7] in the limit $u\ll 1$ if one takes account of the asymptotic power-law behavior of the scaling function $\psi(\omega)\sim\omega^{x_1}$ (see Sec. V), where x_1 is the surface magnetic exponent:

$$G(u)\simeq u^{-kx}\exp\left(-\frac{\pi x_1u^{1-k}}{2C(1-k)}\right). \tag{3.10}$$

Similarly, one can derive an expression for the profile of the local order parameter along the axis of the parabola, when all the border sites are connected to the infinite cluster, from the corresponding profile in the half-plane geometry with fixed boundary conditions. In this latter geometry, the profile $P_\ell(y)$ is given by a power law,

$$P_\ell(y)=Ay^{-x}. \tag{3.11}$$

According to the transformation law

$$P_\ell(w)=b^x(z)P_\ell(z), \tag{3.12}$$

we obtain

$$P_\ell(u)=A\left(\frac{\pi}{2C}\right)^x u^{-kx}\tanh^x\left(\frac{\pi u^{1-k}}{2C(1-k)}\right) \tag{3.13}$$

for the local order parameter for a given origin site $\ell(u,0)$. Intensive numerical simulations of site percolation in the parabolic geometry were performed in order to test the analytical results predicted by conformal invariance.

IV. MONTE CARLO SIMULATIONS FOR PERCOLATION IN TWO DIMENSIONS

We study site percolation on a restricted area A of the square lattice, which is bounded by the curve of equation $v=\pm Cu^k$ and the straight line of equation $u=D$ (Fig. 1). Due to the discretization of space, the continuous curve is approximated by a set Π of points with integer coordinates, $u_p=0,1,\ldots,L$ and $v_p=\pm[Cu_p^k]$, where $[\alpha]$ denotes the integer part of α. Since these points fall either slightly inside or exactly on the continuous curve, they are systematically incorporated into area A.

Site percolation is defined in the usual way: the sites in A are randomly colored black (white) with probability p $(1-p)$ and two nearest-neighbor sites belong to the same percolation cluster if both are black. The algorithm used to grow percolation clusters is now briefly described. Initially, the color of the sites in A is not defined, except for the origin site $\ell(u,v=0)$ which is colored black. One percolation cluster is then constructed iteratively from this growth site. At each iteration, one of the growth sites is chosen and each of its four nearest-neighbor sites is updated according to the following rules.

(i) If it has been previously colored, then it is left unchanged.

(ii) If its color has not been defined yet, it is colored

(1) white with probability $1-p$;

(2) black with probability p and, in this case, it is added to the current list of growth sites.

When all of its four nearest neighbors have been updated, the selected site is removed from the list of growth sites. This process is repeated until the list of growth sites is exhausted (finite cluster) or until a site on the cutoff line $u=D$ becomes a growth site ("infinite cluster"), as illustrated in Fig. 2.

This algorithm was used to grow percolation clusters for different p values above and below the percolation threshold of the infinite square lattice, $p_c=0.592\,746\,0\pm 0.000\,000\,5$ [19]. The fact that detailed information about the "infinite" clusters, i.e., clusters that reach the cutoff length, is not required, allowed us to increase significantly the speed of our algorithm for $p>p_c$. In practice, the current growth site was systematically chosen to be the one closest to the cutoff line, $u=D$. As a consequence, the arms of the percolation clusters were systematically explored rightward and, for an infinite cluster, the cutoff line was reached much faster than in the case of a random choice for the current growth site. For each p value considered, $N=10^6$ clusters were generated and

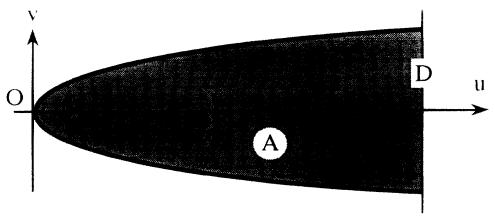

FIG. 1. Representation of the parabolic geometry defined in the text.

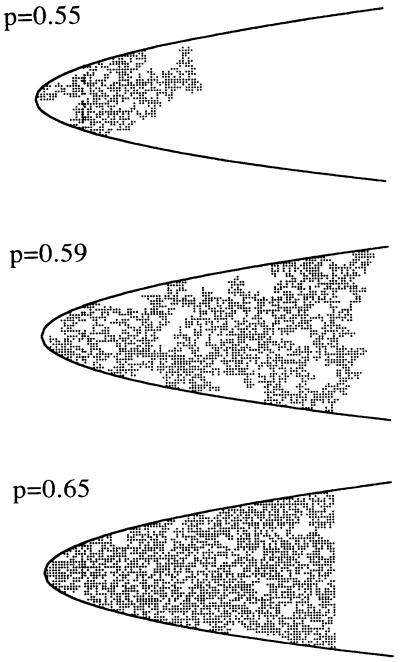

FIG. 2. Typical percolation clusters obtained below p_c (finite cluster), close to and above p_c (infinite clusters) in the parabolic geometry.

the percolation probability $P_\ell(u,p)$ was calculated as

$$P_\ell(u,p) = 1 - \frac{N_f}{N}, \tag{4.1}$$

where N_f is the number of finite clusters grown from the origin site. For $p = p_c$, we also computed the correlation function $G(u)$ as the probability that the origin site $(2,0)$ and a site $(u+2,0)$ belong to the same finite cluster. The number $N - N_f$ of clusters that appear to be infinite necessarily decreases when the cutoff length D is increased. Thus, the estimates of $P_\ell(u,p)$ and $G(u)$ computed for a given D are systematically larger than their asymptotic value reached in the limit $D \to \infty$. The magnitude of this cutoff effect was evaluated in some cases to be discussed in Sec. V.

In a different series of simulations, all the sites on the discretized curve Π were initially colored black, in order to check the predictions of conformal invariance for fixed boundary conditions. With these new boundaries, we computed the u dependence of $P_l(u,p_c)$, the probability that there exists a black cluster which connects the origin site $\ell(u,0)$ to Π. This probability can be obtained by growing a great number of clusters from a seed at a given site $(u,0)$ and by repeating this calculation for any $u \in [1,D]$. We used a more effective way instead. The

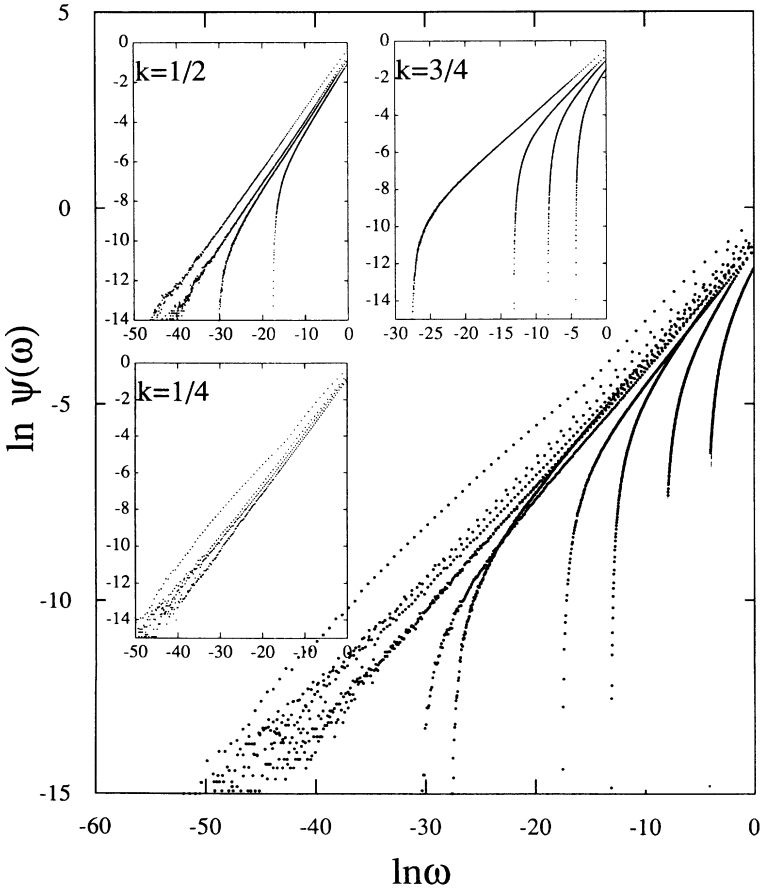

FIG. 3. Log-log plot of the scaling function $\psi(\omega)$ vs ω. The data points correspond to our numerical results for $k = 1/4$, $1/2$, $3/4$ and $C = 1$, 2, 3, and 5 for each value of k. The data for a given k value are displayed separately in inset.

set of black sites in Π was chosen to be the seed and a percolation cluster was grown from it. This way, we got information about $P_\ell(u, p_c)$ for all the u values simultaneously. Here also, $P_\ell(u, p_c)$ is systematically overestimated because of the cutoff at $u = D$. In practice, this bias was observed to be appreciable for u sufficiently close to D and negligible near the tip of the boundary curve.

V. NUMERICAL RESULTS AT THE CRITICAL POINT

The analytical expression derived by using conformal invariance for the correlation function [Eq. (3.9)] can be checked by plotting the scaling function,

$$\psi(\omega) = G(u) \left(\frac{\pi}{2C}\right)^{-2x} u^{kx} \tanh^{-x}\left(\frac{\pi}{2C(1-k)}\right) \times \tanh^{-x}\left(\frac{\pi u^{1-k}}{2C(1-k)}\right), \tag{5.1}$$

as a function of the variable ω which is expressed in terms of the parameters entering the parabolic geometry:

$$\omega = 4\cosh\left(\frac{\pi}{2C(1-k)}\right)\cosh\left(\frac{\pi u^{1-k}}{2C(1-k)}\right) \times \left[\cosh\left(\frac{\pi}{2C(1-k)}\right) - \cosh\left(\frac{\pi u^{1-k}}{2C(1-k)}\right)\right]^{-2}. \tag{5.2}$$

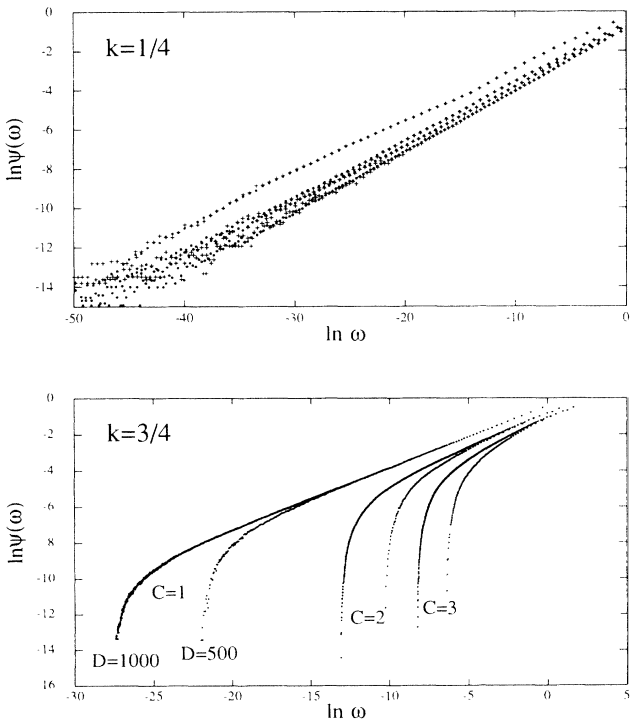

FIG. 4. Same as Fig. 3, with two different cutoff lengths $D_1 = 500$ and $D_2 = 1000$. For $k = 1/4$ there is no detectable effect of the cutoff and the asymptotic regime is reached, while for $k = 3/4$ the finite-size effects are responsible for the deviation from linear behavior.

The bulk magnetic exponent is known to take the value $x = 5/48$. A log-log plot of our numerical data is presented in Fig. 3. Clearly, the scaling function $\psi(\omega)$ appears to be independent of the parameters C and k for large ω values. However, finite-size effects appear as a deviation from the straight line behavior when ω is small. These finite-size effects are more important for wide parabolas (k close to 1 and C large) than for narrow ones as demonstrated by Fig. 4. This figure provides a comparison between the data obtained with two different values of the cutoff D. We observe that, while there is no detectable influence of the cutoff for $k = 1/4$, the cutoff effect is important for $k = 3/4$ and it appears for larger and larger ω values as C is increased. This finite-size effect can be understood easily by noting that for a small cutoff D_1, many clusters which are considered to be infinite (i.e., reach the cutoff line $u = D_1$) are in fact finite as they do not reach the cutoff line $u = D_2 > D_1$.

The straight line behavior observed for the large ω values in Fig. 4 can be related to the asymptotic behavior of the scaling function $\psi(\omega)$. On the semi-infinite system, the correlation function between a point close to the surface ($y_1 \sim 1$) and a point far in the bulk ($y_2 = y$) is expected to decay algebraically at the critical point,

$$G(y) \sim \frac{1}{y^{x+x_1}}. \tag{5.3}$$

Equation (3.8) is in agreement with this form, provided that the scaling function has the following power-law behavior: $\psi(\omega) \sim \omega^{x_1}$. The slope of the log-log plot in Fig. 4 is indeed found to be roughly equal to 0.3, a value

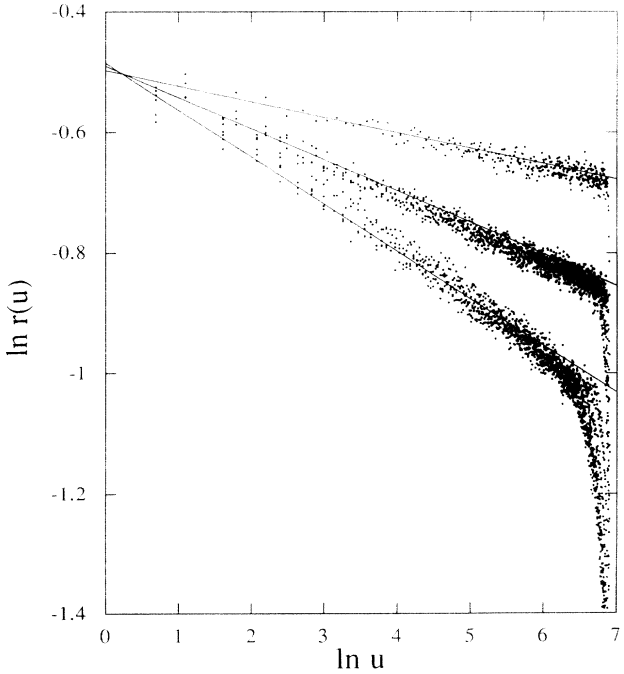

FIG. 5. Log-log plot of $r(u)$ vs u. The data points have been calculated for $C = 1$, 2, 3, and 5 and, from top to bottom, for $k = 1/4$, $1/2$, and $3/4$. The straight lines are linear fits to the data as explained in the text.

which is very close to the expected result $x_1 = 1/3$.

Additional numerical simulations were performed to compute the order parameter profile with fixed boundary conditions. Using Eq. (3.13), we define the reduced parameter

$$r(u) = P_\ell(u)\left[\frac{\pi}{2C}\tanh\left(\frac{\pi u^{1-k}}{2C(1-k)}\right)\right]^{-x}, \qquad (5.4)$$

which must behave like

$$r(u) = Au^{-kx}, \qquad (5.5)$$

where A is a constant which does not depend on k and C. Figure 5 is a log-log plot of our numerical data for $r(u)$ as a function of u for different values of k and C. We observe a straight line behavior in the region where the cutoff effects can be neglected. A linear fit to the data was performed in this region for each value of k. A slope $-kx$ was imposed for the fits, so that the intercept $\ln A$ was the only free parameter. The estimates found for $k = 1/4$, $1/2$, and $3/4$ are $A = 0.608$, 0.612, and 0.616 respectively. We, thus, verify with a great accuracy that A is a constant. Moreover, the imposed slopes $-kx$ clearly fit quite well the data points. A direct comparison of the numerical and analytical profiles for P_ℓ is presented in Fig. 6. The analytical curves were calculated by replacing the prefactor A in Eq. (3.13) by the estimates given above. Here again, we obtain an excellent agreement between the simulation data and the results of conformal invariance.

In the case of free boundary conditions, no analytical expression is known for the local order parameter P_ℓ. However, in analogy with the bulk behavior, we may expect that P_ℓ will scale in the vicinity of the critical threshold.

VI. NUMERICAL RESULTS OFF THE CRITICAL POINT

As discussed in Sec. II, the q-state Potts model with a coupling constant K is equivalent, in the limit $q \to 1$, to percolation with a probability $p = 1 - e^{-K}$. We can, thus, define a reduced temperature,

$$t = \ln\left(\frac{1-p_c}{1-p}\right) \sim K - K_c, \qquad (6.1)$$

as a scaling variable. Let us denote by $P_\ell(u,p)$, the probability that the origin site $\ell(u,0)$ belongs to an infinite cluster. Assuming that P_ℓ is a generalized homogeneous function of u, t and the parabola coefficient C, we have, with the choice $b = t^{-\nu}$ in Eq. (1.2),

$$P_\ell(u,t,C^{-1}) = t^\beta f\left(\frac{u}{\xi}, \frac{R_c}{\xi}\right) = t^\beta f(\lambda,\kappa). \qquad (6.2)$$

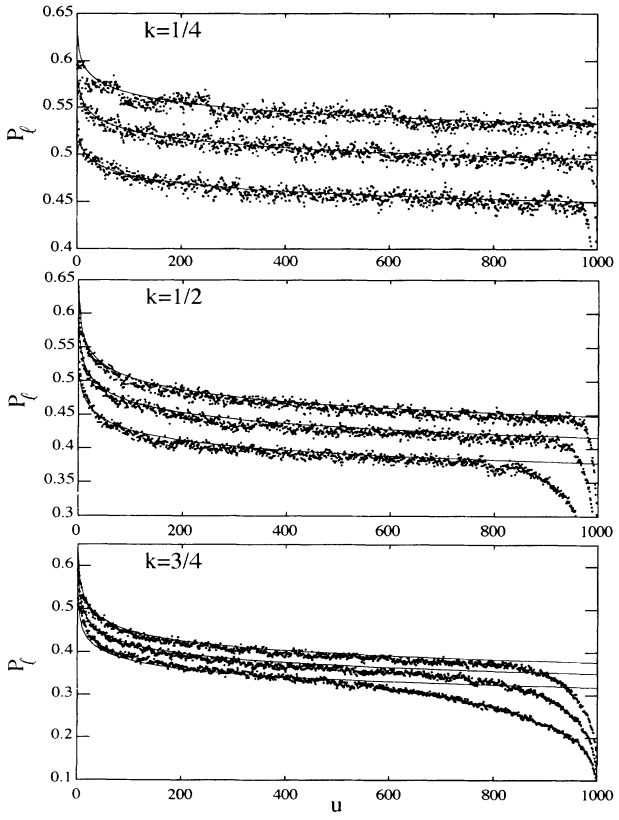

FIG. 6. Numerical (dots) and analytical (lines) results for the magnetization profile. The discrepancy at large u is due to finite-size effects which are more important for wide parabolas. μ is given in lattice spacing units.

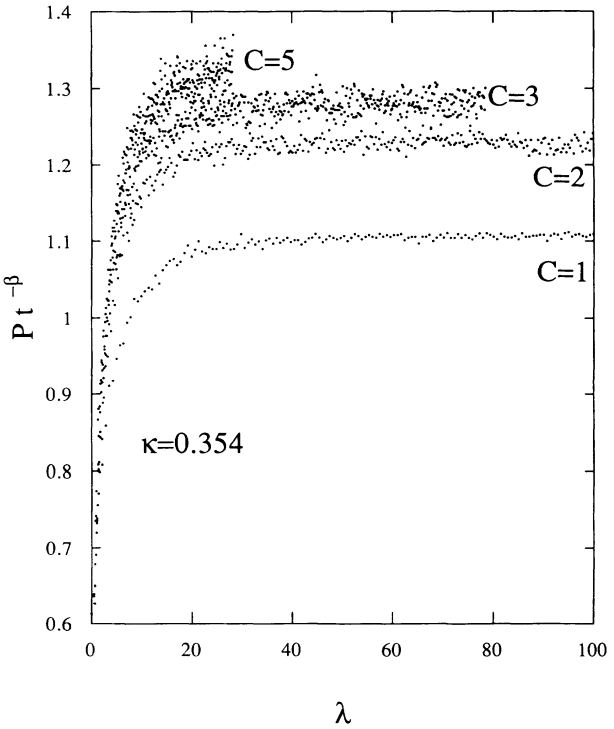

FIG. 7. Nonuniversal behavior of the scaled order parameter $P_\ell t^{-\beta}$ as a function of the reduced abscissa $\lambda = u/\xi$. The parameters are $k = 1/2$, $C = 1$, 2, 3, and 5. For each C value, the temperature t is adjusted so as to keep a fixed ratio $\kappa = R_c/\xi = 0.354$.

In this equation, $\xi \sim t^{-\nu}$ represents the bulk correlation length with its exponent $\nu = 4/3$, $R_c \sim C^{\frac{1}{1-k}}$ the characteristic length associated with the parabolic geometry and $\beta = 5/36$ is the critical exponent for the percolation probability in the bulk.

Keeping the ratio $\kappa = \frac{R_c}{\xi}$ constant, we thus expect that a plot of $P_\ell t^{-\beta}$ as a function of $\lambda = \frac{u}{\xi}$ will give a universal curve. However, our numerical results for P_ℓ do not follow the expected scaling behavior (Fig. 7). This deviation from a universal behavior may be due either to finite-size effects or to correction terms which do not appear in Eq. (6.2). The first possibility is definitely ruled out by comparing the $P_\ell(u)$ profiles computed with two values of the cutoff length, $D = 1000$ and 2000, since the corresponding profiles are identical for $u \leq 1000$, within numerical accuracy. To test the second possibility, we introduce an extra term in Eq. (6.2) which reads now

$$P_\ell(u, t, C^{-1}) = t^\beta f(\lambda, \kappa)\,[1 + t^\epsilon g(\lambda, \kappa)]\,. \tag{6.3}$$

Far from the tip of the parabola, i.e. for $\lambda \to \infty$, the scaling functions f and g assume constant values f_∞ and g_∞ independent of κ, k, and C, since P_ℓ is asymptotic to $P_\infty \sim t^\beta$ which is the bulk percolation probability. As a consequence, Eq. (6.3) reduces to

$$P_\infty = t^\beta f_\infty (1 + t^\epsilon g_\infty). \tag{6.4}$$

Figure 8 is a plot of $y = \ln P_\infty - \beta \ln t$ as a function of t in the case $k = 1/2$. The values for P_∞ were computed for different values of C and t by averaging the corresponding profiles $P_\ell(u)$ in the range $u \in [1800, 2000]$. A least-squares fit of the data points to a curve of equation $y = A + \ln(1 + Bt^\epsilon)$ gives

$$\epsilon = 0.179 \pm 0.016. \tag{6.5}$$

This result confirms our assumption that the corrections to the simple scaling behavior given in Eq. (6.2) are substantial. Now that ϵ is known, we can use Eq. (6.3) to determine the correction function g. We again keep κ fixed and allow λ to vary. Equation (6.3) gives then

$$P_\ell(u_1, t_1, C_1^{-1}) = t_1^\beta f(\lambda_1)\,[1 + t_1^\epsilon g(\lambda_1)] \tag{6.6}$$

and

$$P_\ell(u_2, t_2, C_2^{-1}) = t_2^\beta f(\lambda_2)\,[1 + t_2^\epsilon g(\lambda_2)] \tag{6.7}$$

for two independent systems which are off the critical point. With the choice $u_1 t_1^\nu = u_2 t_2^\nu$, the same λ value is recovered on both systems and we obtain

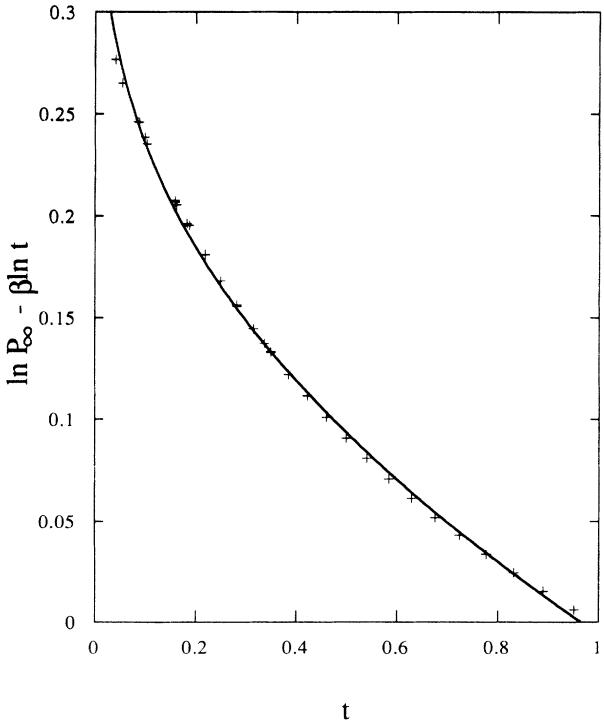

FIG. 8. A least-squares fit (line) to the curve $y = A + \ln(1 + Bt^\epsilon)$ of the numerical data (+) for $y = \ln P_\infty - \beta \ln t$ as a function of t. The parameters are $k = 1/2$, $C = 1$, 2, 3, and 5.

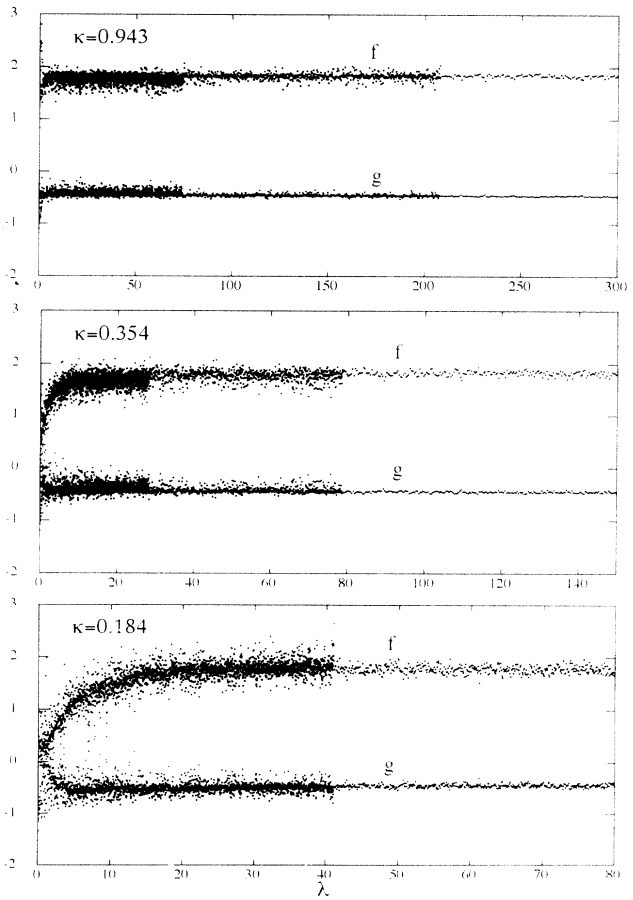

FIG. 9. The scaling function f and the correction to scaling function g plotted as functions of the reduced abscissa $\lambda = u/\xi$. The parameters are $k = 1/2$, $C = 1$, 2, 3 and 5, and the temperatures are chosen in order to get fixed ratios $\kappa = R_c/\xi = 0.943$, 0.354, and 0.184. The asymptotic values f_∞ and g_∞ in the bulk (λ large) appear to be constants independent of k, C, and t.

$$g(\lambda) = \frac{T_{1,2} - 1}{t_1^{\epsilon} - t_2^{\epsilon} T_{1,2}}, \tag{6.8}$$

where

$$T_{1,2} = \left(\frac{t_2}{t_1}\right)^{\beta} \frac{P_\ell(u_1, t_1, C_1^{-1})}{P_\ell(u_2, t_2, C_2^{-1})}. \tag{6.9}$$

Finally, we compute the scaling function f as

$$f(\lambda) = \frac{P_\ell(u_1, t_1, C_1^{-1}) t_1^{-\beta}}{1 + t_1^{\epsilon} g(\lambda)} = \frac{P_\ell(u_2, t_2, C_2^{-1}) t_2^{-\beta}}{1 + t_2^{\epsilon} g(\lambda)}. \tag{6.10}$$

In practice, $f(\lambda)$ was taken to be the average of these two expressions. The numerical data obtained for $\kappa = 0.184$, 0.354, and 0.943 confirm the above analysis (see Fig. 9). We indeed verify our basic assumption that f_∞ and g_∞ are constants. We also observe that $g(\lambda)$ can be approximated by a constant, $g_\infty \simeq -0.452$, with good precision. The crucial test of Eq. (6.3) is now to plot

$$\frac{P_\ell(u, t, C^{-1}) t^{-\beta}}{1 + t^{\epsilon} g_\infty} \tag{6.11}$$

as a function of λ and to check that a universal curve is obtained. This test was successful, as can be seen in Fig. 10. As a consequence, the scaling assumption given in Eq. (6.3) is confirmed.

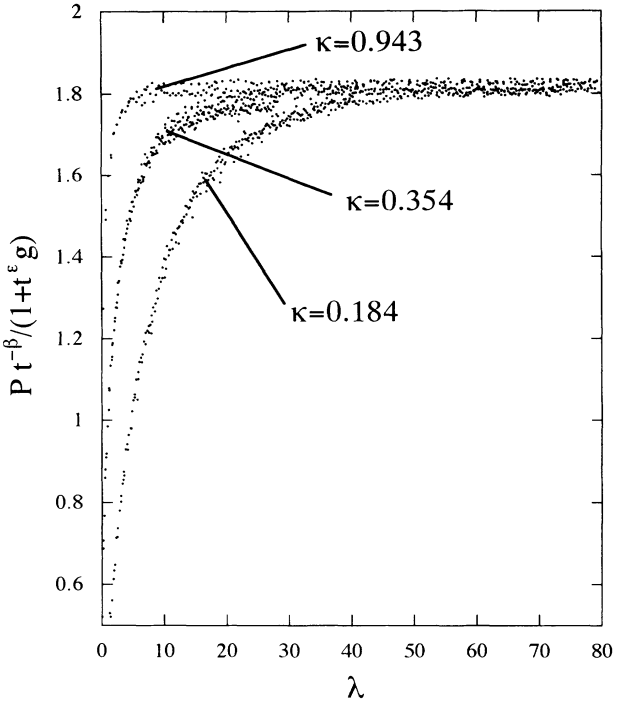

FIG. 10. Universal behavior of the scaled order parameter including correction to scaling, $P_\ell t^{-\beta}/(1+t^{\epsilon} g_\infty)$, as a function of $\lambda = u/\xi$. The parameters are $k = 1/2$, $C = 1$, 2, 3, and 5, and $\kappa = R_c/\xi = 0.943$, 0.354, and 0.184.

VII. SUMMARY

Confined systems are known to display critical behaviors which may depend on the geometry. In this paper, we have investigated the case of the site percolation problem for a two-dimensional system limited by a parabolic surface. Scaling arguments show that this shape corresponds to a relevant geometric perturbation. We have performed intensive Monte Carlo simulations at the critical point for the tip-bulk correlation function. Our numerical results are in agreement with an analysis using conformal invariance. The correlation function along the axis of the parabola exhibits a stretched exponential behavior as already encountered for other confined models. The order parameter profile has been computed at the critical point for fixed boundary conditions. The data again are in excellent agreement with the analytic expression of the profile deduced from the conformal mapping. Finally we have analyzed the off-critical order parameter profile including corrections to scaling. The leading correction to scaling exponent has been estimated and it was shown that the correction to scaling function $g(\lambda)$ does not vary significantly.

ACKNOWLEDGMENTS

We are indebted to Loïc Turban for stimulating this work and for interesting discussions. B.B. wishes to thank Ingo Peschel for communicating his work prior to publication. H.-P.E. thanks the Laboratoire de Physique du Solide for the hospitality extended to him in Nancy, Princeton University for financial support, and the Alexander von Humbolt Foundation. He also acknowledges the stimulating atmosphere of the Aspen Center for Physics, where the last corrections to the paper were made. This work was supported by the Group CNI/Mat (Calcul Numérique Intensif en sciences des Matériaux) under Grant No. 155C93b. The Laboratoire de Physique du Solide is Unité de Recherche Associée au CNRS No. 155.

[1] J.L. Cardy, Nucl. Phys. B **240** [FS12], 514 (1984).
[2] M.N. Barber, I. Peschel, and P.A. Pearce, J. Stat. Phys. **37**, 497 (1984).
[3] C. Kaiser and I. Peschel, J. Stat. Phys. **54**, 567 (1989).
[4] I. Peschel, L. Turban, and F. Iglói, J. Phys. A **24**, L1229 (1991).
[5] M.N. Barber, in *Phase Transitions and Critical Phenomena*, edited by C. Domb and J.L. Lebowitz (Academic Press, London, 1983), Vol. 8, p. 145.
[6] S. Blawid and I. Peschel, Z. Phys. B **95**, 73 (1994).
[7] F. Iglói, I. Peschel, and L. Turban, Adv. Phys. **42**, 683 (1993).

[8] L. Turban and B. Berche, J. Phys. (Paris) **3**, 925 (1993).
[9] L. Turban, J. Phys. A **25**, L127 (1992).
[10] F. Iglói, Phys. Rev. A **45**, 7024 (1992).
[11] C. Kaiser and L. Turban, J. Phys. A **27**, L579 (1994).
[12] P.W. Kasteleyn and C.M. Fortuin, J. Phys. Soc. Jpn. Suppl. **26**, 11 (1969).
[13] F.Y. Wu, J. Stat. Phys. **18**, 115 (1978).
[14] F.Y. Wu, Rev. Mod. Phys. **54**, 235 (1982).
[15] M.R. Giri, M.J. Stephen, and G.S. Grest, Phys. Rev. B **16**, 4971 (1977).
[16] H. Kunz and F.Y. Wu, J. Phys. C **11**, L1 (1978).
[17] R.F. Baxter, *Exactly Solved Models in Statistical Mechanics* (Academic Press, London, 1982).
[18] J.L. Cardy, in *Phase Transitions and Critical Phenomena*, edited by C. Domb and J.L. Lebowitz (Academic Press, London, 1987), Vol. 11, p. 55.
[19] R.M. Ziff, Phys. Rev. Lett. **69**, 2670 (1992).

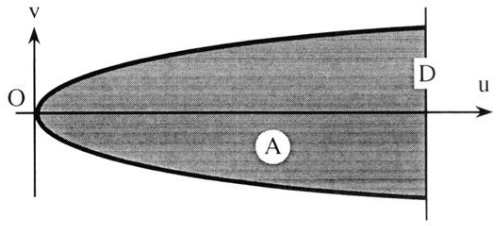

FIG. 1. Representation of the parabolic geometry defined in the text.

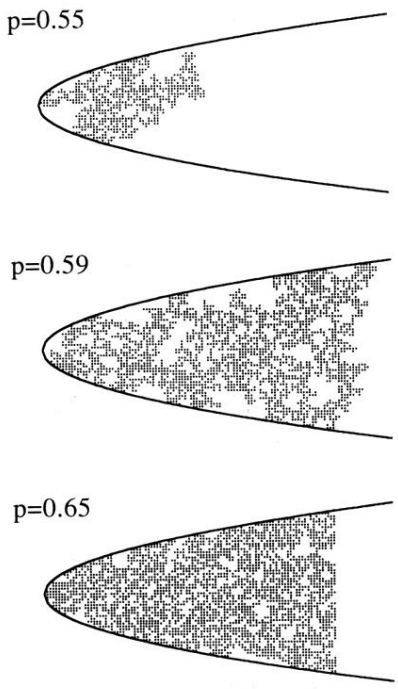

FIG. 2. Typical percolation clusters obtained below p_c (finite cluster), close to and above p_c (infinite clusters) in the parabolic geometry.